Biophysical Chemistry 141 (2009) 124–130

Contents lists available at ScienceDirect

Biophysical Chemistry

journal homepage: http://www.elsevier.com/locate/biophyschem

Backbone conformational dependence of peptide acidity

Janet S. Anderson [a], Griselda Hernández [b], David M. LeMaster [b,*]

[a] Department of Chemistry, Union College, Schenectady, New York 12308, USA
[b] Wadsworth Center, New York State Department of Health and Department of Biomedical Sciences, School of Public Health, University at Albany – SUNY, Empire State Plaza, Albany, New York 12201, USA

ARTICLE INFO

Article history:
Received 12 December 2008
Received in revised form 14 January 2009
Accepted 15 January 2009
Available online 24 January 2009

Keywords:
NMR
Hydrogen exchange
Amide acidity
Peptide conformation
Continuum electrostatics
Dielectric shielding

ABSTRACT

Electrostatic interactions at the protein surface yield over a billion-fold range of amide hydrogen exchange rates. This range is equivalent to the maximal degree of attenuation in exchange rates that have been shown to occur for amides buried within the protein interior. Continuum dielectric analysis of Ala-Ala, Ala-Gly, Gly-Ala and trans-Pro-Ala peptide conformer acidities predicts that the relative orientation of the two neighboring peptide groups can account for a million-fold variation in hydroxide-catalyzed hydrogen exchange rates. As in previous protein studies, an internal dielectric value of 3 was found to be applicable to simple model peptides, presumably reflecting the short lifetime of the peptide anion intermediate. Despite the million-fold range in conformer acidities, the small differences in the experimental exchange rates for these peptides are accurately predicted. Ala-Ala conformers with an extended N-terminal residue and the C-terminal residue in the α conformation are predicted to account for over 60% of the overall hydrogen exchange reaction, despite constituting only 12% of the protein coil population.

1. Introduction

Protein amide hydrogen exchange is commonly interpreted in terms of a conformational protection factor. The ratio of the observed amide exchange rate k_{ex} to the exchange rate for the corresponding local sequence in a model peptide k_{pep} is used to predict the equilibrium constant for the conformational transition by which a structurally buried amide becomes transiently exposed to the solvent phase (i.e., $\Delta G = -RT\ln(k_{ex}/k_{pep})$) [1]. Central to this analysis is the assumption that exposure to solvent results in amide exchange rates that are equal to those for simple model peptides. However, hydrogen exchange measurements for amides that are exposed to solvent in the protein X-ray structure can dramatically conflict with this peptide normalization assumption. The amide hydrogens of *Pyrococcus furiosus* rubredoxin that are solvent-exposed in the 1.1 Å X-ray structure [2] exhibit a billion-fold range of hydroxide-catalyzed exchange rates [3]. In particular, the well exposed (3 $Å^2$) Val 38 amide hydrogen exchanges at a rate that is nearly 10^7-fold slower than that of the corresponding Trp-Val model peptide [4]. Conversely, His 38 in the active site of the **a** domain of the human protein disulfide isomerase exchanges at a rate 400-fold faster than the corresponding model peptide value [5]. Application of the standard protection factor analysis to these two static solvent-exposed amides yields a 13 kcal/mol range of apparent conformational stabilities. This range is at least as large as the maximal global stability of any protein predicted from hydrogen exchange measurements which has been independently verified by either calorimetric or spectroscopic methods [6–8]. Given that these static solvent-exposed amides need not require any conformational transition for hydrogen exchange to occur, it is of interest to explore in detail how the remainder of the protein structure can give rise to such a large range of exchange rates.

Amides are known to react with the hydroxide ion as Eigen [9] normal acids, so that the exchange rate of an amide is equal to the product of the diffusion-limited rate and the fraction of forward-reacting encounters $K_c/(K_c+1)$, where K_c is the equilibrium constant for the transfer of a proton from the amide to an hydroxide ion [10,11]. In turn, electrostatic interactions modulate the acidity of an amide by altering the difference in solvation free energy between the neutral and anionic peptide states [12,13]. In the earlier rubredoxin study [3], Poisson–Boltzmann continuum electrostatic calculations were carried out on the deprotonated peptide form of each static solvent-exposed amide, so as to predict the free energy of proton transfer between these sites. With one exception, the predicted acidities for all of these amides agreed with the observed hydrogen exchange rate constants to within a rmsd of 6 [3].

To analyze the electrostatic contributions to the rate of hydrogen exchange that arise solely from the adjacent peptide units, dipeptide sequences containing only alanine, glycine and proline residues within a large set of high resolution X-ray structures were identified. Continuum dielectric calculations were then carried out on implicitly solvated models of the corresponding N-acetyl-X-X-N-methylamide conformers. By operationally turning off the remainder of the interactions that result from the protein native structure, the contribution to amide acidity that arises from the orientation of the adjacent peptide units can be assessed.

* Corresponding author. Tel.: +1 518 474 6396; fax: +1 518 473 2900.
E-mail address: lemaster@wadsworth.org (D.M. LeMaster).

0301-4622/$ – see front matter © 2009 Elsevier B.V. All rights reserved.
doi:10.1016/j.bpc.2009.01.005

The Protein Coil Library of Rose and coworkers [14] was used to identify target peptide conformers from among the 17,422 protein segments in their library that had been selected from X-ray structures having resolution limits of 1.6 Å and *R* values of 0.25 or better. As for coil libraries in general, the helical and sheet segments of the protein backbones were removed from this Protein Coil Library to yield a set of peptide conformers that are commonly believed to offer the most robust representation presently available for the conformational distribution characteristic of the unstructured protein denatured state and of its constituent peptide components.

Such a conformationally filtered set offers an independent method for assessing the reliability of the proposed peptide conformer electrostatic calculations. In experimental measurements of model peptides, substitution of alanine on either side of the exchange site yields less than a 3-fold change in the amide exchange rate for most sidechain types [4]. However, evidence is presented here which indicates that the orientation of the adjacent peptide units gives rise to a million-fold range in amide acidities for individual conformations that are observed in high resolution protein structures. Yet, despite this wide range of acidities for individual peptide conformers, averaging over the full coil library distribution faithfully predicts the much smaller differences in exchange rates that are observed among simple model peptides.

2. Computational methods

2.1. Continuum dielectric calculations

The 17,422 protein segments selected from X-ray structures having at least 1.6 Å resolution and *R* values of 0.25 or better in the Protein Coil Library of Rose and coworkers [14] were screened for Ala-Ala, Ala-Gly, Gly-Ala, Gly-Gly and trans-Pro-Ala peptides, after the terminal residues of each segment had been excluded so as to further reduce residual conformational bias that could arise from the presence of adjacent regular secondary structure [15]. The Reduce program [16] was used to add hydrogens to the heavy atoms in the backbone segment that extends between the C^{α} atoms on either side of the selected dipeptide, yielding N-acetyl-X-X-N-methylamides. Nonlinear Poisson–Boltzmann calculations were carried out using the DelPhi algorithm [17], with CHARMM22 atomic charge and atomic radius parameters [18]. Except where stated otherwise, the excess charge of the amide anion was localized on the nitrogen atom. This selection reflects the superior performance that was observed for this charge distribution in the present study as well as in previous studies of both model peptide [12] and protein [3] hydrogen exchange. A 0.25 Å grid spacing was used with a 40% filling factor and an ionic radius of 2.0 Å. The external dielectric value was set to 78.5 and an ionic strength of 0.15 M was used, so as to mimic the conditions of our earlier rubredoxin study [3].

2.2. N-methylacetamide modeling

A population of structures for the reference compound N-methylacetamide was generated so as to provide consistency with electrostatic calculations on peptide conformations obtained from the Protein Coil Library. The central peptide unit for each of the Gly-Gly peptides was converted to N-methylacetamide by transformation of the first nitrogen and the last carbonyl carbon to hydrogen atoms. DelPhi calculations were carried out on a lattice grid containing each of these Gly-Gly derived N-methylacetamide molecules with a second N-methylacetamide molecule of fixed geometry. All atoms from each of the two molecules were separated by at least 8 Å. At this distance the variation in the differential electrostatic solvation free energies predicted for the two amide anions was found to be less than 0.1 kT. Assuming an internal dielectric constant value of 3, 68% of the Gly-Gly derived N-methylacetamide molecules had predicted amide pK values within 0.1 units of the mean electrostatic solvation free energy ($\Delta pK = \Delta kT/\ln$ [10]). Averaging over this subpopulation of Gly-Gly derived structures was used to determine an N-methylacetamide reference molecule with C^{α}–C, C–O, C–N and N–C^{α} bond lengths of 1.52, 1.23, 1.33 and 1.45 Å, respectively, and C^{α}–C–O, C^{α}–C–N and C–N–C^{α} bond angles of 120.6°, 116.3° and 121.0°, respectively. These values closely correspond to those for the small molecule X-ray structure [19].

2.3. Crystallographic dipeptide conformer calculations

Electrostatic calculations on the Ala-Ala, Ala-Gly, Gly-Ala and trans-Pro-Ala peptides were carried out similarly with N-methylacetamide added to the box for internal referencing of the differential electrostatic potential. For each peptide conformer, three calculations were carried out: the peptide anion in the presence of the neutral N-methylacetamide; the neutral peptide in the presence of the N-methylacetamide anion; and the neutral peptide in the presence of the neutral N-methylacetamide which serves as the common reference state. In this approach, the coordinates of the reference molecule are not superimposed upon those of the ionizing site of the target molecule in the lattice grid. As a result, incomplete cancellation of the electrostatic self-energy terms can result. To assess the extent of incomplete cancellation, the difference in electrostatic solvation free energy predicted between the neutral and anionic N-methylacetamide molecules for each of the 679 Ala-Ala conformer calculations was found to vary with an rmsd of 0.083 kT, indicating an average grid error of 0.036 pH units in the relative pK values.

3. Results and discussion

In our earlier study of the static solvent-exposed amides in *Pf* rubredoxin [3], the electrostatic solvation free energies of the individual peptide anions were calculated as a function of the force field electrostatic parameter set (CHARMM22 [18], AMBER parm99 [20] and PARSE [21]), the protein internal dielectric constant, and the distribution of the excess negative charge between the amide nitrogen and the carbonyl oxygen of the ionizing peptide linkage. An optimal correlation between the second order rate constants of hydroxide-catalyzed exchange and the predicted differences in the amide pK values was obtained from the use of an internal dielectric value of 3 with the CHARMM22 electrostatic parameter set applied to the peptide anion charge localized on the amide nitrogen. The poorer correlation that was obtained when the excess negative charge of the peptide anion was divided equally between the amide nitrogen and the carbonyl oxygen agrees with the results that were previously reported in continuum dielectric modeling of hydrogen exchange in simple peptides [12].

3.1. Prediction of peptide conformer acidity

In the present study, the optimal electrostatic parameters obtained in our earlier *Pf* rubredoxin study were applied to a set of N-acetyl-Ala-Ala-N-methylamide peptide conformers which were implicitly solvated at 0.15 M ionic strength. A total of 679 Ala-Ala conformations were identified in 17,422 protein segments in the Protein Coil Library [14]. The DelPhi [17] program was used to calculate the electrostatic potential of the central peptide anion for each terminally blocked Ala-Ala conformer, relative to an N-methylacetamide anion reference.

When the CHARMM22 electrostatic parameters were applied to the coil library-derived Ala-Ala peptides with the internal dielectric set to 3, the conformer acidities were found to span a range of 6 pH units (Fig. 1a). A similar range of conformer acidities is predicted for the Ala-Gly peptides (Fig. 1b) as well as for the other coil library peptides considered here. Hence, within the range of conformations observed in native protein structures, the local backbone conformation of the adjacent peptide groups is predicted to give rise to more

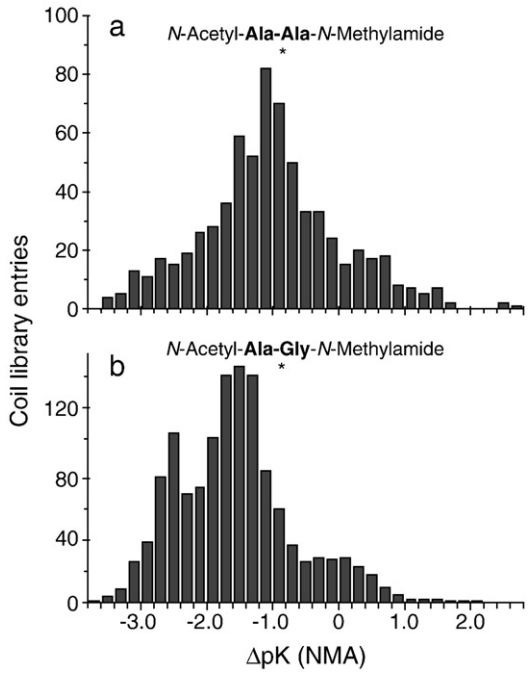

Fig. 1. Peptide acidities of Ala-Ala and Ala-Gly conformers. The electrostatic potential was calculated for the central peptide anion (*) formed from blocked peptides derived from the 679 Ala-Ala (panel a) and 1322 Ala-Gly (panel b) segments found in the Protein Coil Library [14], utilizing the CHARMM22 atomic charge and radius parameters [18] and an internal dielectric value of 3. The N-methylacetamide anion was used as reference.

than a million-fold range in hydroxide-catalyzed amide hydrogen exchange rates. Such effects will not only apply to amides that are solvent-exposed in the folded protein structure. Amides that are buried in the folded protein structure must become exposed to the solvent catalyst in order to undergo hydrogen exchange. When the residual tertiary structure in such an exchange-competent conformation restricts the local backbone conformation surrounding the site of exchange, only a subset of peptide conformer acidities will contribute to the observed exchange.

Analogous continuum dielectric calculations on the ionization of protein sidechains have often predicted far higher dielectric shielding, commonly yielding effective internal dielectric constants near 20 [22,23]. As we have previously noted [3,24], the reduced dielectric shielding observed for the amide ionizations presumably reflects the far shorter lifetime of the peptide anion intermediate. As a result of the highly transient formation of the peptide anion, the conformational relaxation of the protein that can occur in response to this ionized state is severely limited. Since amides are known to act as Eigen normal acids [10,11] and the peptide anion is generally a stronger base than hydroxide, the peptide anion should be quenched by a neutral water molecule at a diffusion-limited rate. Although a direct measurement of the peptide anion quenching reaction has not been reported, NMR relaxation studies indicate that the residence lifetime of an hydroxide ion in water is ~5 ps [25], Lifetimes near 10 ps have commonly been observed for photoactivated strong acids [26,27]. Both of these processes occur at rates similar to the 8 ps time constant for the dominant process of Debye dielectric relaxation of water [28] that primarily arises from reorientation of the water molecules, and it is argued that the dynamics of water reorientation are limiting in these fast proton transfer reactions [26,27]. Although much less extensively studied, the complementary process of proton transfer from neutral water to a photoactivated strong base appears to follow similar kinetics [29], as would be anticipated from the common interpretation that hydroxide transfer through water can be reasonably well represented as a "proton hole" variation of the better-characterized hydronium ion transfer process [30,31].

In contrast, neutral carboxyl, amine and imidazole sidechains react with hydroxide and hydronium ion at diffusion-limited rates, while the reverse process of proton donation to, or removal from, a neutral water molecule occurs at a rate determined by the sidechain pK value. As a result, lifetimes in the range of microseconds to milliseconds occur for these ionized sidechains near neutral pH. During this longer timeframe, extensive dielectric reorganization of the protein can occur in response to a change in the charge state. Indeed, explicit representation of these conformational relaxation processes in the modeling of sidechain titrations reduces the effective level of dielectric shielding down toward the high frequency dielectric limit [32–34] which has ε^{∞} values near 2 for most nonpolar organics and 3.4 for N-methylformamide at 25 °C [35].

As illustrated in Fig. 2, nearly all of the most highly acidic Ala-Ala peptides have the N-terminal residue in either a β (center at $\phi \approx -130°$, $\psi \approx 125°$) or a polyproline II (center at $\phi \approx -80°$, $\psi \approx 145°$) conformation and the C-terminal residue in the α conformation. The reverse pattern holds true for the least acidic peptide conformers. It is the residue with a conformation near the α-helix basin of the Ramachandran map which dominates this behavior. When the C-terminal residue is an α conformation, the positive end of this peptide dipole points toward the ionizing nitrogen, thus stabilizing the anionic intermediate (Fig. 3a). Similarly, the negative end of that peptide dipole points toward the ionizing nitrogen when the N-terminal residue is in an α

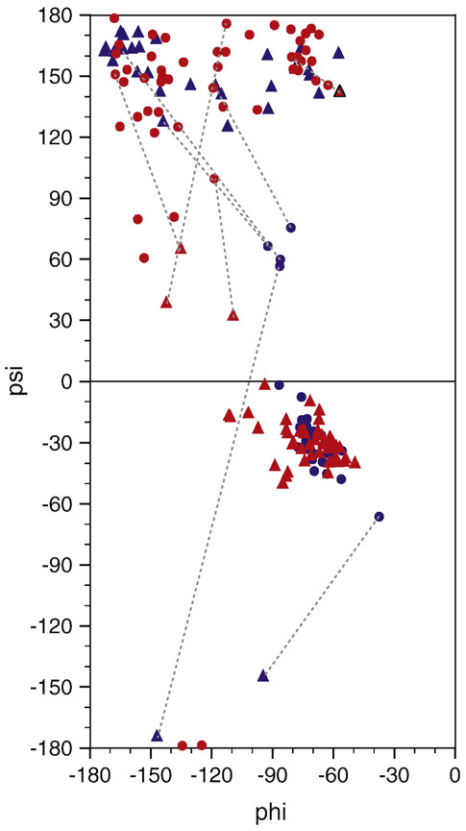

Fig. 2. The backbone conformational distribution of the most acidic and least acidic N-acetyl-Ala-Ala-N-methylamide conformers in the Protein Coil Library. The (ϕ,ψ) torsion angle values for the 50 most acidic peptides are plotted in red, while the values for the 30 least acidic peptides are plotted in blue. The N-terminal residues are denoted by circles and the C-terminal residues by triangles. Dotted lines are used to correlate the N- and C-terminal residue backbone torsion angles for peptides that do not bridge between the extended and α conformational regions. None of the most acidic peptides have positive ϕ torsion angles. The one highly acidic peptide with both residues in a polyproline II conformation (red triangle with black outline – Ala 55 and Ala 56 of pdb code 2DT8) has an intervening peptide linkage with an anomalously small C–N bond length (1.22 Å) and C^{α}–C–N bond angle (105.8°). (For interpretation of the references to colour in this figure legend, the reader is referred to the web version of this article.)

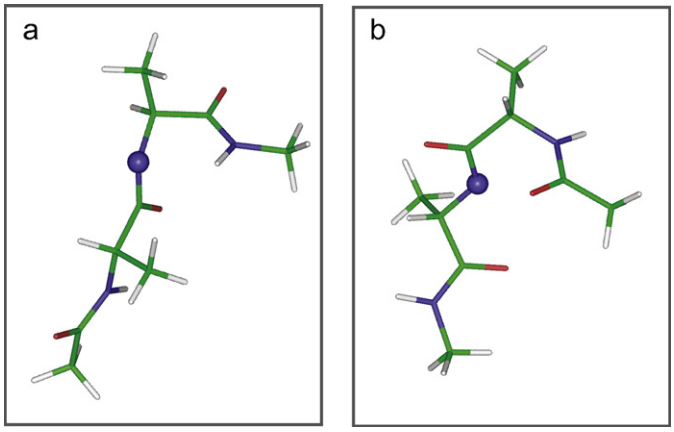

Fig. 3. Conformations of Ala-Ala segments with markedly differing predicted peptide acidities. In panel a is illustrated the backbone structure surrounding Ala 462–Ala 463 from the human cytosolic 5′ nucleotidase (pdb code 2JC9 [49]) with (ϕ,ψ) values of (−165,165) and (−65,−30). The amide H–N bond vector of residue 464 is oriented toward the amide nitrogen of Ala 463, giving rise to an enhanced acidity for that peptide. In panel b is illustrated the backbone structure surrounding Ala 188–Ala 189 from the ebola virus matrix protein VP40 (pdb code 1H2C [50]) with (ϕ,ψ) values of (−61,−35) and (−145,143). The carbonyl O–C bond vector of residue 187 is oriented toward the amide nitrogen of Ala 189, giving rise to a reduced acidity for that peptide.

conformation (Fig. 3b). A similar argument applies to the Ala-Gly peptides. In this case, the wider range of conformations that are energetically accessible to the glycine residue (Fig. 4) permits (ϕ,ψ) torsion angles in the basin near (+90°, 0°) so that the C-terminal peptide dipole is oriented toward the ionizing nitrogen, thus stabilizing the peptide anion. As could be expected, dipeptides in which both residues are either in the α conformation or in the extended conformation have amide acidities near the middle of the pK distribution since the electrostatic interactions of the two terminal peptide groups tend to cancel one another. Junctions in the backbone geometry will tend to give rise to extremes of amide acidity, such as at the N-terminus of an α-helix, in which the peptide linkage at the site of transition between extended and helical conformations is known to undergo rapid hydrogen exchange [36,37].

3.2. Boltzmann averaging of conformer acidities

Despite the million-fold range in amide acidities that is predicted for the Ala-Ala and Ala-Gly peptide conformers, the log difference in the experimental exchange rate that arises from substitution of glycine for the C-terminal alanine is only 0.27 [4]. As seen in Fig. 1, the distribution of the Ala-Gly conformers is predicted to shift toward increased acidities, relative to the Ala-Ala peptide. Indeed, the population-averaged amide pK shifts 0.54 units for the Ala-Gly peptide, a value that is twice the experimentally observed shift. Population averaging of the conformer pK_i values (or, equivalently, averaging the conformer electrostatic potential values) has occasionally been used to estimate the effect of conformer sampling in the prediction of protein sidechain ionization, although population averaging of the conformer acidities (K_i) is more formally correct [38]. In a detailed analysis of sidechain ionizations in bovine pancreatic trypsin inhibitor and hen egg-white lysozyme, Karplus

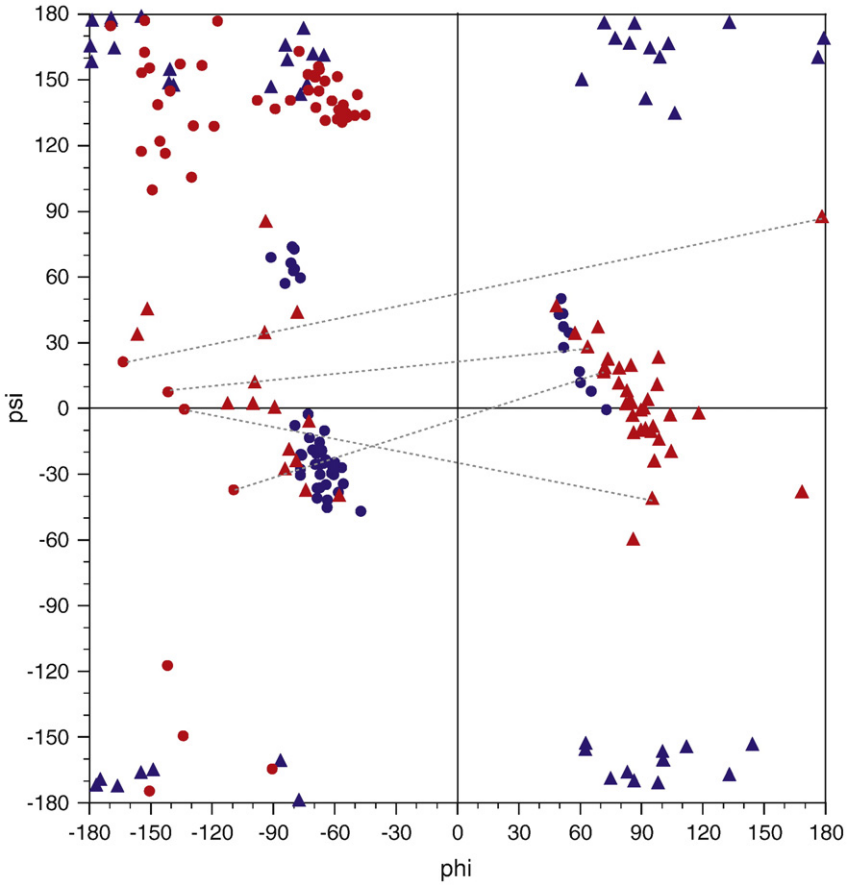

Fig. 4. The backbone conformational distribution of the most acidic and least acidic N-acetyl-Ala-Gly-N-methylamide conformers in the Protein Coil Library. The (ϕ,ψ) torsion angle values for the 50 most acidic (red) and the 50 least acidic (blue) peptides are plotted. The N-terminal residues are denoted by circles and the C-terminal residues by triangles. Those highly acidic peptides that have a pair of (ϕ,ψ) values which lie outside of the dominant pattern connecting N-terminal residues in the extended region to C-terminal residues in either the right- or left-handed α regions are correlated by dotted lines. (For interpretation of the references to colour in this figure legend, the reader is referred to the web version of this article.)

and coworkers [39] concluded that, in assessment of the ionization midpoint for each titrating residue, averaging over the K_i values or averaging over the log K_i values has little effect on the predicted pK values. The principal effect of averaging over a range of acidity values is generally to flatten out the standard Henderson–Hasselbach pH dependence of the proton occupancies, which is typically modeled by introducing a Hill cooperativity coefficient less than 1.0 into the Henderson–Hasselbach equation.

When referenced to the titration midpoint as the operational pK value, the effect from a small subpopulation of a highly acidic conformer is largely independent of the magnitude of that increased acidity, as long as a substantial majority of that conformer is ionized at the midpoint of the full Boltzmann-averaged population. On the other hand, for hydroxide-catalyzed hydrogen exchange near neutral pH only ~1 out of every 10^{10} molecules will have a given amide in the ionized state. As a result, the most acidic conformers can make a dominant contribution to the observed hydrogen exchange rate, despite constituting only a modest fraction of the overall conformer population.

When the conformer acidities are averaged over the coil library populations illustrated in Fig. 1, the amide pK of the Ala-Gly peptide is predicted to be 0.20 less than that of the Ala-Ala peptide, nearly equal to the experimentally observed difference. The smaller difference predicted by the conformer acidity averaging arises from the fact that, although the overall distribution of the Ala-Gly conformers of Fig. 1b clearly shifts to higher acidities as compared to the Ala-Ala peptide in Fig. 1a, the leading edge of the distribution for the most acidic conformers is reasonably similar for the two peptides. Analogous conformer acidity summations for the coil library Gly-Ala and trans-Pro-Ala peptides were also found to offer robust predictions of the corresponding differences in hydroxide-catalyzed hydrogen exchange rates (Table 1).

3.3. The effective internal dielectric shielding for conformer acidity

The predicted range of conformer amide pK values is approximately inversely proportional to the assumed internal dielectric value. In the analysis of the solvent-exposed amides of *Pf* rubredoxin, the choice of an internal dielectric value of either 2 or 4 gave significantly weaker correlations between the observed hydrogen exchange rates and the predicted differences in amide pK values than did the dielectric value of 3 [3]. In contrast, the hydrogen exchange predictions in Table 1 provide a relatively poor test of the effective internal dielectric value, since similar differential hydrogen exchange rates are predicted when the internal dielectric is set to either 2 or 4. In part, this insensitivity to the value of the internal dielectric arises from the onset of diffusion-limited exchange for the most acidic conformers. Amides react with hydroxide ion at a diffusion-limited rate of 2×10^{10} M^{-1} s^{-1} at 25 °C [10,11]. N-methylacetamide has been reported to exchange at a rate 5000-fold below the diffusion limit [10]. Hence, those peptide conformers that are over 5000-fold more acidic than N-methylacetamide will have an upper bound to their reactivity determined by the diffusion-limited rate. For an internal dielectric value of 3, the most acidic Ala-Ala and Ala-Gly conformers just attain that limit (Fig. 1). However, if a dielectric value of 2 is assumed, 1/6 of the Ala-Gly and Gly-Ala conformers are predicted to have reached the diffusion-limited rate of exchange, while only 1/12 of the Ala-Ala conformers are predicted to be so acidic.

Table 1
Hydrogen exchange log rate correction factors (relative to Ala-Ala)

	Experimental [4]	Predicted (ε_{int}=3)
Ala-Gly	0.27	0.20
Gly-Ala	0.17	0.28
transPro-Ala	−0.24	−0.26

A more robust test of the effective internal dielectric value can be obtained from prediction of the experimental difference of 1.82 between the log exchange rate constants for N-methylacetamide and N-acetyl-Ala-Gly-N-methylamide [40]. From the conformer acidities summarized in Fig. 1b, differential log exchange rate constant values of 2.98, 2.17 and 1.61 are predicted for internal dielectric constant values of 2, 3 and 4, respectively. Hence, within the assumptions of this analysis, the effective internal dielectric shielding for the simple peptides appears to be quite similar to that predicted for the solvent-exposed amides of *Pf* rubredoxin.

For the rubredoxin hydrogen exchange study [3], the optimal performance of a low dielectric value appears to be justified by the limited range of backbone motion that can be expected to occur within the timeframe of the ~10 ps lifetime of the peptide anion. Furthermore, unhindered sidechain rotamer transitions generally occur at 10 to 100-fold slower rate [41,42], thus limiting their contribution to dielectric shielding of the peptide anion. On the other hand, conformational mobility is obviously less restricted in the model peptides. Molecular dynamics simulations predict a ~10 ps state lifetime for the transition between the polyproline II and β conformations in model peptides [43], similar to the anticipated lifetime of the peptide anion intermediate. However, the transition from an α conformation to an extended conformation is predicted to occur in ~200 ps [43,44], such that little contribution to the dielectric shielding of the peptide anion can be expected from this transition. Therefore, even in the case of unrestricted peptide mobility, the conformational contribution to dielectric shielding of amide ionization appears to be severely limited.

3.4. Estimation of the acidic peptide conformer population

The (ϕ,ψ) distribution of the most acidic Ala-Ala conformers shown in Fig. 1a is dominated by peptides that have an extended conformation for the N-terminal residue and an α conformation for the C-terminal residue. Within the Protein Coil Library, 85 Ala-Ala conformers lie within the backbone torsion angle range of ($-180°<\phi<-40°$, $\psi>90°$) for the N-terminal residue and ($-90°<\phi<-40°$, $-50°<\psi<0°$) for the C-terminal residue. When the K_i values of these 85 Ala-Ala conformers are summed, relative to the total for all 679 Ala-Ala conformers, this subset of acidic conformers are predicted to account for 62% of the total hydrogen exchange, while constituting only 12% of the population. In contrast, 27% of the Ala-Ala peptides in the coil library have both residues in the extended conformation, yet these conformers account for only 6% of the total hydrogen exchange if the single peptide with distorted bond geometry is excluded (see Fig. 2 legend). Similarly, 25% of the Ala-Ala peptides in the coil library have both residues in a broad α conformation ($-120°<\phi<-40°$, $-60°<\psi<50°$), yet only 5% of the total exchange arise from these conformers. For both the extended–extended and alpha–alpha conformers, the average acidity is 5-fold less than for the full Boltzmann-averaged Ala-Ala peptide population, while in turn the extended–alpha conformer is 5-fold more acidic than that population-averaged value.

A single class of conformers contributes the majority of the hydrogen exchange reaction that occurs for N-acetyl-Ala-Ala-N-methylamide. If the average acidity of that class of conformers can be accurately predicted, the experimentally observed exchange rate can be used to estimate the fractional population of that class of conformers by simply assuming that all of the exchange arises from those conformers. On that basis, 19% of the total population of Ala-Ala conformers would be predicted to have an extended conformation for the N-terminal residue and an α conformation for the C-terminal residue in the present analysis.

Although such an analysis of the fractional population of the dominant acidic conformers may prove to be of some use in characterizing the Boltzmann-weighted conformational distribution in the unstructured peptide state, it is within the context of residual

protein conformational structure that the most significant utility of this analysis can be anticipated. In the simplest instance, whenever the range of peptide acidities within a set of conformers is greater than the range in differential population among these conformers, a single conformer may provide the dominant contribution to the observed exchange behavior. Such an effect can be illustrated in the hydrogen exchange of the static solvent-exposed amides of *Pf* rubredoxin [3]. In the high resolution X-ray structure [2] the sidechain χ_1 torsion angles of Asp 21 and Asp 36 are oriented near −60°, placing the negatively charged carboxylate group within 3 Å of the intraresidue amide hydrogen. The resultant strong interaction with the peptide anion intermediate predicts a far slower hydrogen exchange rate than is experimentally observed. Taking advantage of the fact that the X-ray structure presents little hindrance to rotation of those sidechains into the trans conformation, electrostatic potential calculations for those trans conformations predicted hydrogen exchange rates that were 10^3 and 10^5-fold faster than for the gauche χ_1 sidechain conformers of Asp 21 and Asp 36, respectively [3]. The amide acidities predicted for the trans conformers of these two aspartates closely match their observed hydrogen exchange rates, indicating that for these two residues the enhanced acidity of the trans sidechain conformation should dominate the observed exchange behavior.

Most informative may be the case of the structurally buried amide for which exchange-competent conformations are only rarely accessed. If such exchange-competent conformations can be realistically modeled, then the prediction of the peptide acidity in those conformational states will allow the free energy of the underlying conformational transition to be estimated without the need to invoke the potentially dubious assumption that hydrogen exchange kinetics are independent of the surrounding conformational structure.

4. Conclusion

In general, a protein amide cannot be accurately assumed to exchange at model peptide rates unless that segment of the backbone samples a range of conformations which approximates the distribution of conformations in the unstructured state. When the remainder of the protein structure restricts conformational sampling, a potentially large range of amide acidities can arise. While the present study is focused on the electrostatic contributions that arise from the adjacent peptide units, it must be emphasized that structural analysis of the billion-fold range in exchange rates for the static solvent-exposed amides of *Pf* rubredoxin clearly indicates that a much larger set of electrostatic interactions within the protein structure can significantly contribute to the variations in peptide acidity [3].

Prediction of the differential hydrogen exchange rates for model peptides depends upon the accuracy of the conformer distribution used to represent the Boltzmann-weighted sampling. Characterization of the Boltzmann distribution of model peptide conformers in solution continues to be a major challenge [45–47]. The importance of this problem is underscored by the fact that the peptide conformer distribution serves as the reference state for analysis of residual structure in unfolded proteins. In turn, proper characterization of the unfolded state bears upon the wide range of pathologies that arise from protein misfolding [48]. The degree to which the present results accurately predict experimental peptide exchange values provides support for the suitability of the Protein Coil Library [14] as a model for unstructured peptide conformations, particularly with respect to the actively debated question regarding the relative fraction of the unfolded state that resides in the α conformation as opposed to in the extended conformation [45–47].

The electrostatic modulation of amide exchange kinetics renders the analysis dependent upon modeling the conformational structure surrounding the site of exchange. However, conversely, by dispensing with the conventional assumption that the chemistry of exchange is insensitive to the residual tertiary structure, electrostatic analysis may offer a pathway to characterization of the structure of the transient exchange-competent state.

References

[1] Y.W. Bai, J.S. Milne, L. Mayne, S.W. Englander, Protein stability parameters measured by hydrogen exchange, Proteins: Struct., Funct., Genet. 20 (1994) 4–14.
[2] R. Bau, D.C. Rees, D.M. Kurtz, R.A. Scott, H.S. Huang, M.W.W. Adams, M.K. Eidsness, Crystal-structure of rubredoxin from *Pyrococcus furiosus* at 0.95 Angstrom resolution, and the structures of N-terminal methionine and formylmethionine variants of Pf Rd. Contributions of N-terminal interactions to thermostability, J. Biol. Inorg. Chem. 3 (1998) 484–493.
[3] J.S. Anderson, G. Hernández, D.M. LeMaster, A billion-fold range in acidity for the solvent-exposed amides of *Pyrococcus furiosus* rubredoxin, Biochemistry 47 (2008) 6178–6188.
[4] Y.W. Bai, J.S. Milne, L. Mayne, S.W. Englander, Primary structure effects on peptide group hydrogen-exchange, Proteins: Struct., Funct., Genet. 17 (1993) 75–86.
[5] G. Hernández, J.S. Anderson, D.M. LeMaster, Electrostatic stabilization and general base catalysis in the active site of the human protein disulfide isomerase **a** domain monitored by hydrogen exchange, ChemBioChem 9 (2008) 768–778.
[6] S.E. Radford, M. Buck, K.D. Topping, C.M. Dobson, P.A. Evans, Hydrogen exchange in native and denatured states of hen egg-white lysozyme, Proteins 14 (1992) 237–248.
[7] B.M.P. Huyghes-Despointes, J.M. Scholtz, C.N. Pace, Protein conformational stabilities can be determined from hydrogen exchange rates, Nat. Struct. Biol. 6 (1999) 910–912.
[8] J. Hollien, S. Marqusee, Comparison of the folding processes of *T. thermophilus* and *E. coli* Ribonucleases H, J. Mol. Biol. 316 (2002) 327–340.
[9] M. Eigen, Proton transfer, acid-base catalysis, and enzymatic hydrolysis. (I) Elementary processes, Angew. Chem., Int. Ed. 3 (1964) 1–19.
[10] R.S. Molday, R.G. Kallen, Substituent effects on amide hydrogen exchange rates in aqueous solution, J. Am. Chem. Soc. 94 (1972) 6739–6745.
[11] W.H. Wang, C.C. Cheng, General base catalyzed proton exchange in amides, Bull. Chem. Soc. Jpn. 67 (1994) 1054–1057.
[12] F. Fogolari, G. Esposito, P. Viglino, J.M. Briggs, J.A. McCammon, pKa shift effects on backbone amide base-catalyzed hydrogen exchange rates in peptides, J. Am. Chem. Soc. 120 (1998) 3735–3738.
[13] F. Avbelj, R.L. Baldwin, Origin of the neighboring residue effect on peptide backbone conformation, Proc. Natl. Acad. Sci. U.S.A. 101 (2004) 10967–10972.
[14] N.C. Fitzkee, P.J. Fleming, G.D. Rose, The protein coil library: a structural database of nonhelix, nonstrand fragments derived from the PDB, Proteins: Struct., Funct., Genet. 58 (2005) 852–854.
[15] L.L. Perskie, T.O. Street, G.D. Rose, Structures, basins, and energies: a deconstruction of the Protein Coil Library, Prot. Sci. 17 (2008) 1151–1161.
[16] J.M. Word, S.C. Lovell, J.S. Richardson, D.C. Richardson, Asparagine and glutamine: using hydrogen atom contacts in the choice of side-chain amide orientation, J. Mol. Biol. 285 (1999) 1733–1747.
[17] W. Rocchia, S. Sridharan, A. Nicholls, E. Alexov, A. Chiabrera, B. Honig, Rapid grid-based construction of the molecular surface and the use of induced surface charge to calculate reaction field energies: applications to the molecular systems and geometric objects, J. Comput. Chem. 23 (2002) 128–137.
[18] A.D. MacKerell, D. Bashford, M. Bellott, R.L. Dunbrack Jr., J.D. Evanseck, M.J. Field, S. Fischer, J. Gao, H. Guo, S. Ha, D. Joseph-McCarthy, L. Kuchnir, K. Kuczera, F.T.K. Lau, C. Mattos, S. Michnick, T. Ngo, D.T. Nguyen, B. Prodhom, W.E. Reiher, B. Roux, M. Schlenkrich, J.C. Smith, R. Stote, J. Straub, M. Watanabe, J. Wiorkiewicz-Kuczera, D. Yin, M. Karplus, All-atom empirical potential for molecular modeling and dynamics studies of proteins, J. Phys. Chem. B 102 (1998) 3586–3616.
[19] F. Hamzaoui, F. Baert, X-ray study of static disorder in N-methylacetamide, Acta Crystallogr., C Cryst. Struct. Commun. 50 (1994) 757–759.
[20] T.E. Cheatham, P. Cieplak, P.A. Kollman, A modified version of the Cornell et al. force field with improved sugar pucker phases and helical repeat, J. Biomol. Struct. Dyn. 16 (1999) 845–862.
[21] D. Sitkoff, K.A. Sharp, B. Honig, Accurate calculation of hydration free energies using macroscopic solvent models, J. Phys. Chem. 98 (1994) 1978–1988.
[22] J. Antosiewicz, J.A. McCammon, M.K. Gilson, The determinants of pKa's in proteins, Biochemistry 35 (1996) 7819–7833.
[23] E. Demchuk, R.C. Wade, Improving the continuum dielectric approach to calculating pKa's of ionizable groups in proteins, J. Phys. Chem. 100 (1996) 17373–17387.
[24] D.M. LeMaster, J.S. Anderson, G. Hernández, Spatial distribution of dielectric shielding in the interior of *Pyrococcus furiosus* rubredoxin as sampled in the subnanosecond timeframe by hydrogen exchange, Biophys. Chemist. 129 (2007) 43–48.
[25] Z. Luz, S. Meiboom, The activation energies of proton transfer reactions in water, J. Am. Chem. Soc. 86 (1964) 4768–4769.
[26] L.M. Tolbert, K.M. Solntsev, Excited-state proton transfer: from constrained systems to "super" photoacids to superfast proton transfer, Acc. Chem. Res. 35 (2002) 19–27.
[27] P. Leiderman, L. Genosar, D. Huppert, Excited-state proton transfer: indication of three steps in the dissociation and recombination process, J. Phys. Chem. A 109 (2005) 5965–5977.
[28] W.J. Ellison, K. Lamkaouchi, J.M. Moreau, Water: a dielectric reference, J. Mol. Liq. 68 (1996) 171–279.
[29] H.J. Park, O.H. Kwon, C.S. Ah, D.J. Jang, Excited-state tautomerization dynamics of 7-hydroxyquinoline in β-cyclodextrin, J. Phys. Chem. B 109 (2005) 3938–3943.
[30] D. Asthagiri, L.R. Pratt, J.D. Kress, M.A. Gomez, Hydration and mobility of HO^-(aq), Proc. Natl. Acad. Sci. U.S.A. 101 (2004) 7229–7233.
[31] M.E. Tuckerman, A. Chandra, D. Marx, Structure and dynamics of OH^-(aq), Acc. Chem. Res. 39 (2006) 151–158.

[32] P.E. Smith, R.M. Brunne, A.E. Mark, W.F. vanGunsteren, Dielectric properties of trypsin inhibitor and lysozyme calculated from molecular dynamics, J. Phys. Chem. 97 (1993) 2009–2014.
[33] T. Simonson, D. Perahia, Internal and interfacial dielectric properties of cytochrome c from molecular dynamics in aqueous solution, Proc. Natl. Acad. Sci. U.S.A. 92 (1995) 1082–1086.
[34] T. Simonson, C.L. Brooks III, Charge screening and the dielectric constant of proteins: insight from Molecular dynamics, J. Am. Chem. Soc. 118 (1996) 8452–8458.
[35] J. Barthel, R. Buchner, B. Wurm, The dynamics of liquid formamide, N-methylformamide, N-N-dimethylformamide. A dielectric relaxation study, J. Mol. Liq. 98–99 (2002) 51–69.
[36] H.J. Dyson, A. Holmgren, P.E. Wright, Assignment of the protein NMR spectrum of reduced and oxidized thioredoxin – sequence specific assignments, secondary structure and global fold, Biochemistry 28 (1989) 7074–7087.
[37] J. Kemmink, N.J. Darby, K. Dijkstra, R.M. Scheek, T.E. Creighton, Nuclear magnetic resonance characterization of the N-terminal thioredoxin-like domain of protein disulfide isomerase, Protein Sci. 4 (1995) 2587–2593.
[38] T.J. You, D. Bashford, Conformation and hydrogen ion titration of proteins: a continuum electrostatic model with conformational flexibility, Biophys. J. 69 (1995) 1721–1733.
[39] H.W.T. vanVlijmen, M. Schaefer, M. Karplus, Improving the accuracy of protein pKa calculations: conformational averaging versus the average structure, Proteins: Struct., Funct., Genet. 33 (1998) 145–158.
[40] R.S. Molday, S.W. Englander, R.G. Kallen, Primary structure effects on peptide group hydrogen exchange, Biochemistry 11 (1972) 150–158.
[41] D.M. LeMaster, NMR relaxation order parameter analysis of the dynamics of protein sidechains, J. Am. Chem. Soc. 131 (1999) 1726–1742.
[42] N.R. Skrynnikov, O. Millet, L.E. Kay, Deuterium spin probes of side-chain dynamics in proteins. 2. Spectral density mapping and identification of nanosecond time-scale side-chain motions, J. Am. Chem. Soc. 124 (2002) 6449–6460.
[43] Y. Mu, D.S. Kosov, G. Stock, Conformational dynamics of trialanine in water 2. Comparison of AMBER, CHARMM, GROMOS, and OPLS force fields to NMR and Infrared experiments, J. Phys. Chem. B 107 (2003) 5064–5073.
[44] M.H. Zaman, M.Y. Shen, R.S. Berry, K.F. Freed, T.R. Sosnick, Investigations into sequence and conformational dependence of backbone entropy, inter-basin dynamics and the Flory isolated-pair hypothesis for peptides, J. Mol. Biol. 331 (2003) 693–711.
[45] J. Makowska, S. Rodziewicz-Motowidto, K. Baginska, J.A. Vila, A. Liwo, L. Chmurzynski, H.A. Scheraga, Polyproline II conformation is one of many local conformational states and is not an overall conformation of unfolded peptides and proteins, Proc. Natl. Acad. Sci. U.S.A. 103 (2006) 1744–1749.
[46] K. Chen, Z. Liu, C. Zhou, W.C. Bracken, N.R. Kallenbach, Spin relaxation enhancement confirms dominance of extended conformations in short alanine peptides, Angew. Chem., Int. Ed. 46 (2007) 9036–9039.
[47] J. Graf, P.H. Nguyen, G. Stock, H. Schwalbe, Structure and dynamics of the homologous series of alanine peptides: a joint molecular dynamics/NMR study, J. Am. Chem. Soc. 129 (2007) 1179–1189.
[48] X. Fernandez-Busquets, N.S. deGroot, D. Fernandez, S. Ventura, Recent structural and computational insights into conformational diseases, Curr. Med. Chem. 15 (2008) 1336–1349.
[49] K. Wallden, P. Stenmark, T. Nyman, S. Flodin, S. Graslund, P. Loppnau, V. Bianchi, P. Nordlund, Crystal structure of human cytosolic 5′-nucleotidase II: Insights into allosteric regulation and substrate recognition, J. Biol. Chem. 282 (2007) 17828–17836.
[50] F.X. Gomis-Ruth, A. Dessen, J. Timmins, A. Bracher, L. Kolesnikowa, S. Becker, H.D. Klenk, W. Weissenhorn, The matrix protein VP40 from Ebola virus octamerizes into pore-like structures with specific RNA binding properties, Structure 11 (2003) 423–433.